

Structures of $\text{Cl}^-(\text{H}_2\text{O})_n$ and $\text{F}^-(\text{H}_2\text{O})_n$ ($n=2,3,\dots,15$) clusters: Molecular dynamics computer simulations

Lalith Perera and Max L. Berkowitz

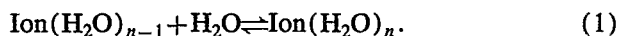
Department of Chemistry, University of North Carolina, Chapel Hill, North Carolina 27599

(Received 27 August 1993; accepted 21 October 1993)

We have performed molecular dynamics calculations on $\text{Cl}^-(\text{H}_2\text{O})_n$ and $\text{F}^-(\text{H}_2\text{O})_n$ ($n=2,3,\dots,15$) clusters. The calculations show that the F^- ion is solvated in these clusters, while Cl^- remains attached to the water in the clusters. We also obtained the minimum energy structures for the $\text{Cl}^-(\text{H}_2\text{O})_n$ and $\text{F}^-(\text{H}_2\text{O})_n$ ($n=6,7,8$) clusters. From the comparison of these structures with the dynamical structures we conclude that the solvation of the F^- ion is due to the entropy effect.

I. INTRODUCTION

The study of hydration of ions by few water molecules provides important information for our understanding of solvation phenomena. This study received a new impetus due to recent experimental and theoretical work on this subject.¹⁻²³ The first experimental data on these systems were obtained by Kebarle and co-workers.^{1,2} Using mass spectroscopic techniques they measured the temperature dependence of the equilibrium constants K for the reaction,



Once the temperature dependence of the equilibrium constant is known, the heat of the reaction (1) can be obtained from the Van't Hoff equation,

$$\Delta H_{n-1,n}^0 = -R \frac{\partial(\ln K)}{\partial(1/T)} \quad (2)$$

In its turn the knowledge of the heat of reaction (1) can be used to test the quality of the interaction potentials between the ion and water molecules. Unfortunately the experimental measurements of the heats of reaction (1) could be performed only for very small sized clusters (with up to $n=8$ water molecules), thus limiting our testing abilities of the quality of the potential. Moreover, from the knowledge of the heat of the reaction it is hard to extract information on the structure of the clusters. Recently an improvement in the experimental situation has occurred due to the application of photoelectron spectroscopy techniques to anion-water clusters.¹⁰ Prior to its use on the halide-water clusters photoelectron spectroscopy demonstrated its value in the study of the electron solvation in water clusters where it allowed one to perform a comparison between calculations and experiment.^{24,25}

As of today we have available to us data from the photodetachment spectra of the following clusters: $\text{Cl}^-(\text{H}_2\text{O})_n$ ($n=1,\dots,7$); $\text{Br}^-(\text{H}_2\text{O})_n$ ($n=1,\dots,15$), and $\text{I}^-(\text{H}_2\text{O})_n$ ($n=1,\dots,15$).²⁶ Very recently we have demonstrated that the experimental stabilization energies (E_{stab}) for I^- , and Br^- and the calculated stabilization energies for Cl^- in these clusters satisfy the relationship

$$E_{\text{stab}} = Cf(n), \quad (3)$$

where $f(n)$ is a universal function that depends only on the number of water molecules in the cluster and C is the proportionality constant.²⁷ The existence of the relationship described by Eq. (3) means that the structures of calculated $\text{Cl}^-(\text{H}_2\text{O})_n$ and experimental $\text{X}^-(\text{H}_2\text{O})_n$ ($n=2,\dots,15$, $\text{X}=\text{Br}, \text{I}$) clusters are similar.²⁸ And since we observed in our simulations that the Cl^- ion is located on the surface of these water clusters, from the similarity argument we therefore concluded that Br^- and I^- ions are not solvated by water clusters either.

As far as the clusters with Cl^- are concerned we observe the following: (a) Our calculated stabilization energies for $\text{Cl}^-(\text{H}_2\text{O})_n$ ($n=2,\dots,7$) clusters are in a good agreement with the experiment. (b) The experimental E_{stab} (for all the available experimental data) in $\text{Cl}^-(\text{H}_2\text{O})_n$ ($n=1,2,\dots,7$) clusters fit the universal curve. (c) The quantum mechanical calculations performed on $\text{Cl}^-(\text{H}_2\text{O})_{14}$ cluster indicate the preference for the Cl^- ion to be on the surface of the water cluster.²⁹

All these factors in our opinion provide support to the previously proposed conjecture that the Cl^- ion is also located on the surface of the water clusters which contain up to 20 water molecules.^{30,31} Nevertheless, the final judgment on the location of Cl^- in these clusters should be given only after the photodetachment experiment will be performed.

Considering the previously given information about the structure of halide anion/water clusters it is therefore interesting to find out which properties of the ion influence the structure of these clusters. In our previous study of the $\text{Cl}^-(\text{H}_2\text{O})_{20}$ cluster we observed that the polarizability of the ion does not substantially change the structure of the cluster, but the sign of the ionic charge has a profound influence on the structure.³¹ Another ionic property that may have a dramatic effect on the cluster structure is the ion size. To study the dependence of the cluster structure on the ionic size we could change the ion-water potential in such a way that only the size of the ion would change, and study the effect of this change. Instead we decided to study a realistic system of the $\text{F}^-(\text{H}_2\text{O})_n$ clusters and compare the results with the results from our calculations on $\text{Cl}^-(\text{H}_2\text{O})_n$ clusters. In this way we can also complete our study of structural properties of small water clusters ($n < 15$) with embedded halogen ions.

TABLE I. Potential parameters used in the present study.

	O-O	O-Cl ⁻	O-F ⁻
$A \times 10^5$ (\AA^{12} kcal/mol)	6.36	37.90	7.21
C (\AA^6 kcal/mol)	627.95	1373.84	712.63
	O	H	Cl ⁻
$ q $	0.730	0.365	1.0
α (\AA^3)	0.465	0.135	3.250
		Cl ⁻	F ⁻
$B \times 10^5$ (kcal/mol)		8.00	2.75
β (\AA^{-1})		2.25	2.25
γ (\AA^{-1})		0.25	0.25

II. METHODS

A. Potentials

To describe the halide ion-water and water-water interactions we used the POL1 potential model which includes many-body effects.²¹⁻²³ In this model the water molecule is assumed to have three charges placed at the positions of two hydrogens and the oxygen. The Lennard-Jones center is placed on the oxygen site. The OH distance in the model is 1 \AA and the HOH angle is 109.47°. Three polarizable centers are placed at each atomic site in water. The ion in this model is considered to be a point charge placed at a Lennard-Jones center. Additionally a polarization center is also placed at the same location.

The total energy of the system is given by the following expression:

$$U_{\text{tot}} = U_{\text{el}} + U_{\text{LJ}} + U_{\text{pol}} + U_{3\text{-body}}, \quad (4)$$

where

$$U_{\text{el}} = \sum_{i < j} q_i q_j / r_{ij} \quad (5)$$

is the sum of all Coulomb interactions between all i and j charge sites and

$$U_{\text{LJ}} = \sum_{\alpha < \beta} (A_{\alpha\beta} / r_{\alpha\beta}^{12} - C_{\alpha\beta} / r_{\alpha\beta}^6) \quad (6)$$

is the sum of the Lennard-Jones interactions between α and β Lennard-Jones sites. The polarization energy is obtained from the expression

$$U_{\text{pol}} = \sum_{i < j} \mu_i \cdot \mathbf{T}_{ij} \cdot \mu_j - \sum_i q_i \sum_j \frac{\mu_j \cdot \mathbf{r}_{ij}}{|\mathbf{r}_{ij}|^3} + \sum_i \frac{\mu_i^2}{2\alpha_i}, \quad (7)$$

where α_i is the polarizability, μ_i is the induced dipole at the polarizable i th center, and \mathbf{r}_{ij} is the distance vector from site i to site j . The values of the induced dipoles at the polarizable centers are calculated self-consistently using relationships (8) and (9),

$$\mu_i = \alpha_i \mathbf{E}_i, \quad (8)$$

$$\mathbf{E}_i = \mathbf{E}_i^0 - \sum \mathbf{T}_{ij} \cdot \mu_j, \quad (9)$$

TABLE II. Calculated (MD) and experimental (expt.) heats of formation of $\text{X}^-(\text{H}_2\text{O})_n$ clusters in kcal/mol.

n	Cl ⁻ (MD)	Cl ⁻ (expt.) ^b	F ⁻ (MD)	F ⁻ (expt.) ^b
2	27.7	27.7	45.5	42.5
3	40.1	39.5	61.8	57.8
4	49.9	50.1	73.6	71.7
5	58.4	59.6	86.2	84.0
6	70.0	68.4	96.4	94.9
7	79.4	76.5 ^a	109.1	105.3
8	90.5	...	118.7	116.5
9	99.7	...	128.5	127.6
10	106.7	...	138.4	138.6 ^a
11	118.4	...	147.8	...
12	128.0	...	157.3	...
13	138.6	...	167.4	...
14	150.7	...	177.3	...
15	157.3	...	185.7	...

^aValues are the best estimates.

^bReference 4.

where \mathbf{E}_i is the total electrostatic field at the i th center and \mathbf{E}_i^0 is the field due to permanent charges. The dipole tensor \mathbf{T}_{ij} in Eq. (9) is

$$\mathbf{T}_{ij} = 1/r_{ij}^3 (\mathbf{I} - 3\mathbf{r}_{ij}\mathbf{r}_{ij}/r_{ij}^2). \quad (10)$$

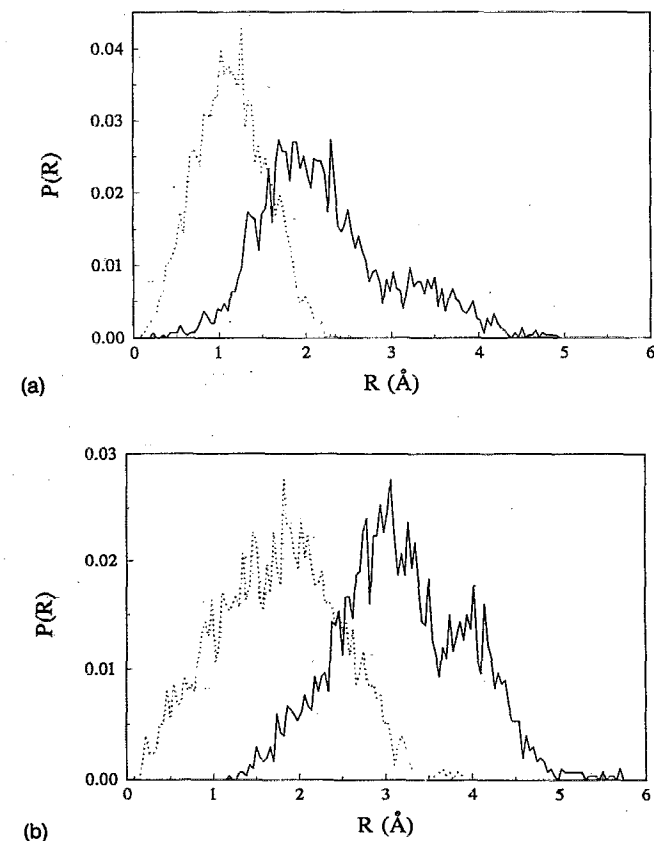


FIG. 1. (a) The distribution of distances from the ion to the center of mass of the cluster. Solid line is for the $\text{Cl}^-(\text{H}_2\text{O})_7$ cluster; dotted for the $\text{F}^-(\text{H}_2\text{O})_7$ cluster. (b) The same as (a), only for the clusters with 15 water molecules.

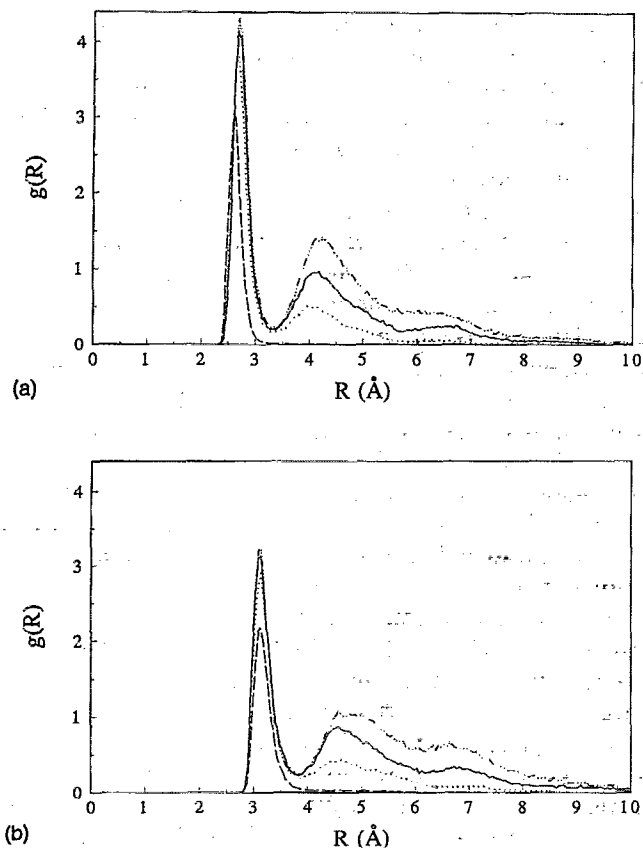


FIG. 2. (a) The ion-water oxygen radial distribution function for $\text{F}^-(\text{H}_2\text{O})_n$ clusters. Dashed line is for the cluster with $n=3$, dotted line is for $n=7$, solid line is for $n=11$, and dot-dashed line is for $n=15$. (b) The same as (a), only for $\text{Cl}^-(\text{H}_2\text{O})_n$ clusters.

The potential energy due to the three body exchange repulsion of the ion-water trimer is expressed in terms of ion-oxygen distances r_{ij} and r_{ik} , and the oxygen-oxygen distance r_{jk} ,

$$U_{3\text{-body}} = B \exp(-\beta r_{ij}) \exp(-\beta r_{ik}) \exp(-\gamma r_{jk}), \quad (11)$$

where B , β , and γ are parameters. The potential parameters of the POL1 model used in the present work are given in Table I.

B. Molecular dynamics

We used molecular dynamics computer simulations to investigate the structure and dynamics of small clusters made up of one ion and n water molecules. Equations of motion were solved using the Verlet algorithm.³² The geometries of the water molecules at their equilibrium values were constrained through the Shake procedure.³³ To solve self-consistent Eqs. (8) and (9) an iterative approach was used. The iterations were continued until the root mean square of the difference in the induced dipoles between successive iterations was <0.001 D/atom. The self-consistency was usually achieved in seven steps of iteration.

Each cluster was initially equilibrated for more than 20 ps followed by 1 ns of the production run. The time step of the trajectory has been kept at 1 fs and the total linear and

angular momenta of the system were removed. During the trajectory calculations the energy was conserved within the 5th significant digit.

All the trajectory calculations were done with the occasional rescaling of the velocities so that the temperature of the clusters was kept constant. For the very small clusters ($n < 4$) the temperature was kept around 275 K, for the clusters with $5 < n < 9$ the temperature was around 250 K. For the clusters with $9 < n < 15$ the average temperature was dropped to around 225 K. The temperature of the clusters was chosen to be high enough to eliminate possible trapping of the cluster in a certain configuration for a very long time. We attempted to perform some molecular dynamics simulations of our clusters at 300 K, but observed the evaporation of water molecules at this temperature.

III. RESULTS

To test the quality of the potential used in the simulation we calculated the heats of cluster formation for $\text{X}^-(\text{H}_2\text{O})_n$ ($\text{X}=\text{Cl}, \text{F}; n=2,3,\dots,15$) clusters and compared these with the experimental data when these were available. The results of such a comparison are given in Table II. As we can see from the table the agreement is rather good, considering the uncertainties in the experiment and in the simulations. To obtain information on the structures of the clusters we calculated (a) distributions of the distances between the ion and the center of mass of the

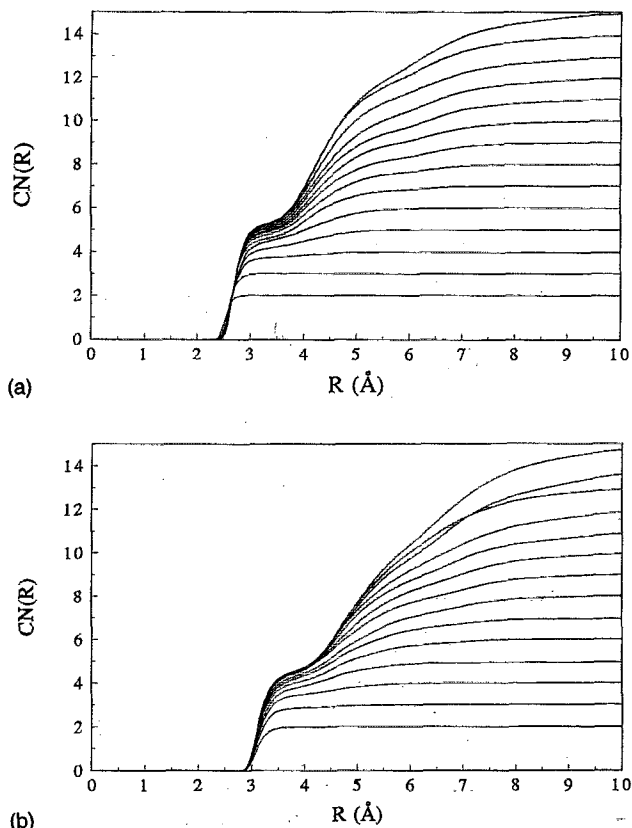


FIG. 3. (a) The running coordination number for the $\text{F}^-(\text{H}_2\text{O})_n$ ($n=2,3,\dots,15$) clusters. (b) The same as (a), only for $\text{Cl}^-(\text{H}_2\text{O})_n$ clusters.

water molecules in the cluster; (b) ion-water oxygen radial distribution functions (rdf) and running coordination number (cn) for an ion in water clusters; (c) angular distribution functions (adf) for each ion in water clusters. We have also examined the snapshots of cluster configurations obtained from our runs. All the data from our calculations lead to the following conclusion: While the Cl^- ion is not solvated in water clusters with up to 15 water molecules, the F^- ion is solvated in the water clusters with $n > 4$.

To justify our conclusion, let us first consider the distribution of the distances from the ion to the center of mass of the cluster. We represent such a distribution for clusters with 7 water molecules in Fig. 1(a). While for the F^- ion the average distance between the ion and the center of mass of the cluster is 1.14 Å, for the Cl^- ion this distance is 1.78 Å. Figure 1(b) presents the distribution of the distances from the ions to the centers of mass of clusters with 15 water molecules. In this case for the F^- ion the average distance between the ion and the center of mass of the cluster is 2.22 Å, while for the Cl^- ion this distance is now 3.19 Å. Figures 1(a) and 1(b) indicate that the F^- ion is more solvated by water clusters than the Cl^- ion. In Fig. 2(a) we represent the ion-oxygen radial distribution functions for clusters with the F^- ion and in Fig. 2(b) ion-oxygen rdf for the clusters with the Cl^- ion. For the clarity of the figures we consider the rdf's for the clusters with 3,

7, 11, and 15 water molecules only. As we can see from the figures, although some similarity exists between the F^- -oxygen and Cl^- -oxygen radial distribution functions, the rdf for Cl^- -oxygen displays a more pronounced third solvation shell is formed around this ion. As to the position of the first peak of the rdf we observed that it is shifting towards the larger distances when the rdf of the F^- ion is considered, while such shift becomes insignificant for clusters with more than five waters when the Cl^- ion is in the cluster. This indicates that the continuous build-up of the solvation shell occurs around F^- , while around Cl^- the first neighbors shell is completed rather early in the growth of the cluster. This also indicates that the F^- ion is solvated, while Cl^- is not. Additional confirmation of this conclusion is provided from the plots of running coordination numbers, depicted in Fig. 3(a) (for F^-) and Fig. 3(b) (for Cl^-). Note that while the coordination number for the first solvation shell is constantly increasing for F^- , until it reaches the value of 5.7 in the cluster with 15 waters, the coordination number for Cl^- approaches the value of 4.4 when 10 water molecules are in the cluster. Direct information about the asymmetry of clusters is given by angular distribution functions³¹ which are presented in Figs. 4(a) and 4(b). For the cluster where the ion is surrounded by waters from all the sides the distribution should look flat. A distinct asymmetry in distribution is observed for the clusters with the Cl^- ion, while the distribution is approaching a flat character for the $\text{F}^-(\text{H}_2\text{O})_{15}$ cluster. (Again, for the matter of clarity, we present the distribution functions for clusters with 3, 7, 11, and 15 waters only.) Finally, snapshots depicting configurations of the clusters with seven water molecules and the corresponding ions are presented in Figs. 5(a) and 5(b).

Now, since we know that F^- is solvated in water clus-

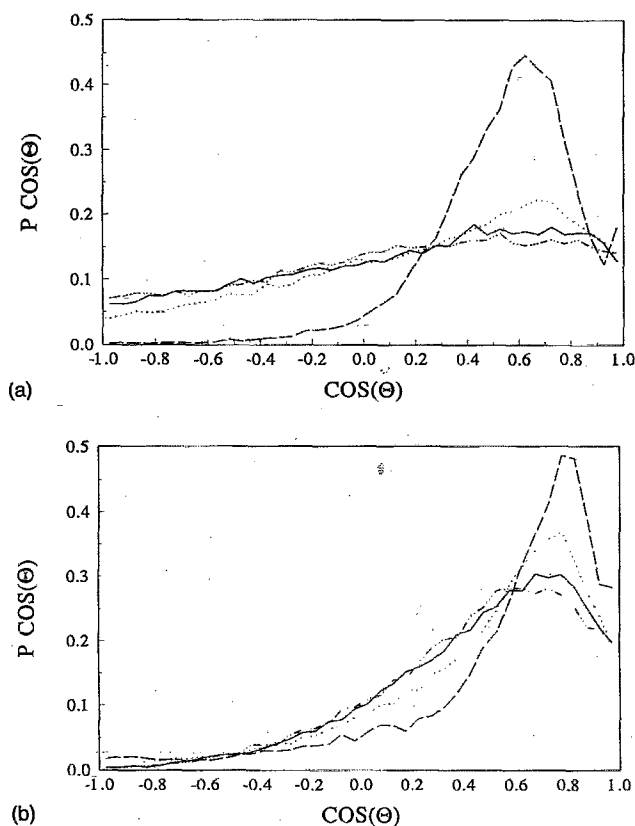


FIG. 4. (a) The angular distribution function for $\text{F}^-(\text{H}_2\text{O})_n$ clusters. Dashed line is for the cluster with $n=3$, dotted line is for $n=7$, solid line is for $n=11$, and dot-dashed line is for $n=15$. (b) The same as (a), only for $\text{Cl}^-(\text{H}_2\text{O})_n$ clusters.

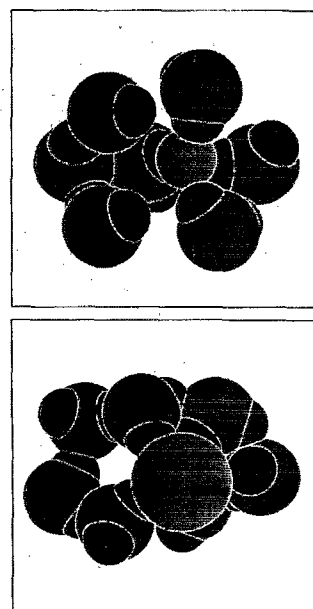


FIG. 5. A snapshot from a trajectory for the $\text{F}^-(\text{H}_2\text{O})_7$ cluster (top) and $\text{Cl}^-(\text{H}_2\text{O})_7$ cluster (bottom).

TABLE III. Total energies and their components in kcal/mol.

n	$-E_{\text{tot}}$	$-E_{\text{pair}}$	$-E_{\text{pol}}$	(a) $\text{Cl}^-(\text{H}_2\text{O})_n$				
				$E_{3\text{-b}}$	$-E_{\text{ww,el}}$	$E_{\text{ww,LJ}}$	$-E_{\text{wi,el}}$	$E_{\text{wi,LJ}}$
2	26.6	21.1	5.7	0.2	0.3	0.2	27.2	6.2
3	38.2	31.0	7.8	0.6	1.0	0.8	38.7	7.9
4	47.8	38.8	9.8	0.8	3.1	1.8	46.6	9.1
5	56.9	46.2	11.7	1.0	6.5	3.3	54.1	11.1
6	66.4	54.1	13.5	1.2	10.4	4.9	60.3	11.7
7	76.9	63.1	15.1	1.3	15.1	6.6	65.4	10.8
8	86.5	70.7	17.2	1.4	21.0	8.7	69.7	11.3
9	95.2	78.0	18.7	1.5	26.2	10.5	73.8	11.5
10	104.3	85.0	20.8	1.5	34.0	13.1	75.7	11.6
11	113.0	92.1	22.5	1.6	40.3	15.2	78.7	11.7
12	121.9	99.1	24.5	1.7	48.8	17.9	80.0	11.8
13	132.0	106.7	27.0	1.7	58.8	21.0	80.8	11.9
14	143.7	116.1	29.3	1.7	67.6	23.8	84.3	12.0
15	149.9	120.8	30.8	1.7	74.8	26.0	83.9	11.9

n	$-E_{\text{tot}}$	$-E_{\text{pair}}$	$-E_{\text{pol}}$	(b) $\text{F}^-(\text{H}_2\text{O})_n$				
				$E_{3\text{-b}}$	$-E_{\text{ww,el}}$	$E_{\text{ww,LJ}}$	$-E_{\text{wi,el}}$	$E_{\text{wi,LJ}}$
2	44.2	31.1	14.3	1.2	-0.8	0.1	46.3	14.3
3	60.0	46.8	15.6	2.4	-2.0	0.2	64.1	15.1
4	71.3	58.9	15.6	3.2	-2.2	0.6	76.5	14.8
5	83.2	70.2	16.6	3.6	0.5	2.2	86.7	14.8
6	92.8	79.9	16.9	4.0	2.1	3.2	95.6	14.6
7	105.6	91.6	18.6	4.6	6.8	5.2	105.0	15.0
8	114.8	99.7	19.9	4.8	11.3	7.0	110.4	15.0
9	124.2	108.0	21.1	5.0	16.4	8.9	115.5	14.9
10	133.4	115.4	23.1	5.1	23.6	11.4	118.3	15.1
11	142.4	123.4	24.3	5.3	29.5	13.4	122.2	14.9
12	151.2	130.2	26.4	5.4	37.4	16.0	123.8	15.0
13	161.0	138.7	27.9	5.6	45.0	18.4	126.8	14.7
14	170.3	146.0	29.9	5.6	54.2	21.3	127.8	14.7
15	178.2	152.7	31.2	5.7	60.2	23.3	130.3	14.5

ters and Cl^- is not, we can ask why this is happening. The energy component analysis which is given in Tables III(a) and III(b) may help us in providing some clues. For the energy component analysis we divided the total energy E_{tot} into the corresponding contributions from the pair interaction energy E_{pair} , polarization energy E_{pol} , and from the 3-body term, $E_{3\text{-body}}$, so that

$$E_{\text{tot}} = E_{\text{pair}} + E_{\text{pol}} + E_{3\text{-body}} \quad (12)$$

In its turn the pair interaction energy can be written as a sum of water-water and water-ion interaction energies; these can be divided into Lennard-Jones and electrostatic parts,

$$E_{\text{pair}} = E_{\text{ww,el}} + E_{\text{ww,LJ}} + E_{\text{wi,el}} + E_{\text{wi,LJ}} \quad (13)$$

where $E_{\text{ww,el}}$ is the electrostatic part of the water-water pairwise interaction, $E_{\text{ww,LJ}}$ is the Lennard-Jones part of the water-water pairwise interaction, $E_{\text{wi,el}}$ is the electrostatic part of the ion-water pairwise interaction, and $E_{\text{wi,LJ}}$ is the Lennard-Jones part of the water-ion pairwise interaction. As Tables III show, a major difference in the energies for F^- and Cl^- is observed for the $E_{\text{wi,el}}$ entry. This energy is lower for clusters with the F^- ion, which may be due to the fact that the F^- is more solvated. It may be also due to the fact that the F^- ion is smaller in size than the Cl^- ion. That the F^- is more solvated than the Cl^- ion can be seen by the inspection of another component of the energy, $E_{\text{ww,el}}$, which is lower for the clusters with the Cl^-

ion. This indicates that the hydrogen bonded network of water is less disturbed by the presence of the Cl^- ion, i.e., the Cl^- ion is less solvated.

Another very interesting fact that can be observed from Tables III is that the relative contribution of the polarization energy into the total energy of the cluster is continuously diminishing (from $\sim 33\%$ for $n=2$ to $\sim 18\%$ for $n=15$) for the clusters with the F^- ion, while for the clusters with the Cl^- ion the relative contribution of the polarization energy remains around the same ($\sim 20\%$). That may mean that it is important to include the polarization effect when the structures of the Cl^- /water clusters are calculated. To see the effect of the explicit inclusion of the polarization into the calculational scheme we represent in Fig. 6 the values of the dipole moments for water molecules as the function of their location in the solvation shells. As we can see the value of the dipole moment of the water molecule is the largest when the molecule is next to the ion and becomes smaller when it is in the next two shells. The values of the dipoles on the water molecules is larger when they are around F^- , again due to the large field emanating from the ion.

To see how the hydrogen bonding pattern changes when water is around the ion in the cluster we calculate the percentage of 0, 1, 2, 3, 4, and 5 hydrogen bonded water molecules in the first and other shells. The histograms representing these percentages are shown in Figs. 7 and 8. As

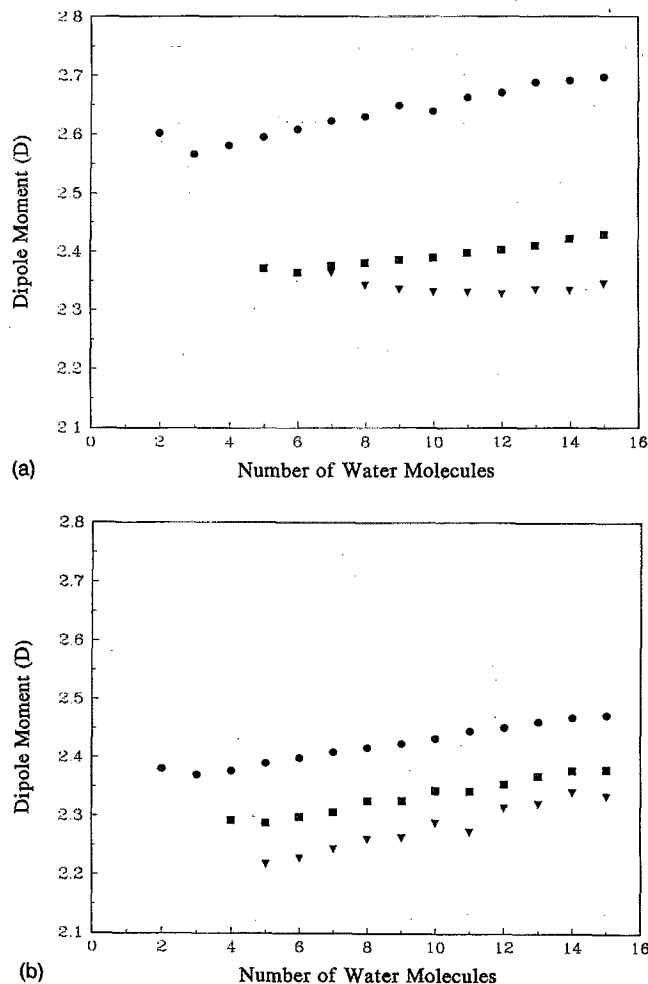


FIG. 6. (a) The values of the total dipole moment of water molecules for the waters in the first solvation shell (circles), second solvation shell (squares), and third solvation shell (triangles), in the $\text{F}^-(\text{H}_2\text{O})_n$ ($n=2,3,\dots,15$) clusters. (b) The same as (a), only for $\text{Cl}^-(\text{H}_2\text{O})_n$ clusters.

we can see from these figures, the first shell water molecules are non-hydrogen bonded in the $\text{F}^-(\text{H}_2\text{O})_n$ clusters with n up to five waters; the one-hydrogen bonded waters are dominant in the clusters with n greater than 6 but less than 14; the two-hydrogen bonded water is the dominant mode in clusters with 14 and 15 water molecules. For the $\text{Cl}^-(\text{H}_2\text{O})_n$ clusters the first shell water molecules are not hydrogen bonded only in the clusters with n up to two waters; the one-hydrogen bonded waters are dominant in the clusters with n from 3 to 10; the one-hydrogen bonded molecules are found as often as two in clusters with $n=11$ and 12 waters; finally the two-hydrogen bonded water is the dominant mode in clusters with 13 to 15 water molecules. For the second shell water molecules the difference in the hydrogen bonding pattern is not that pronounced; for the $\text{F}^-(\text{H}_2\text{O})_n$ and $\text{Cl}^-(\text{H}_2\text{O})_n$ clusters with $n=2,3,\dots,9$ the most often found are water molecules with one hydrogen bond per molecule. Two hydrogen bonds are the most dominant mode for molecules in larger size clusters with the F^- ion. In clusters with the Cl^- ion two-hydrogen bonded molecules dominate in the secondary

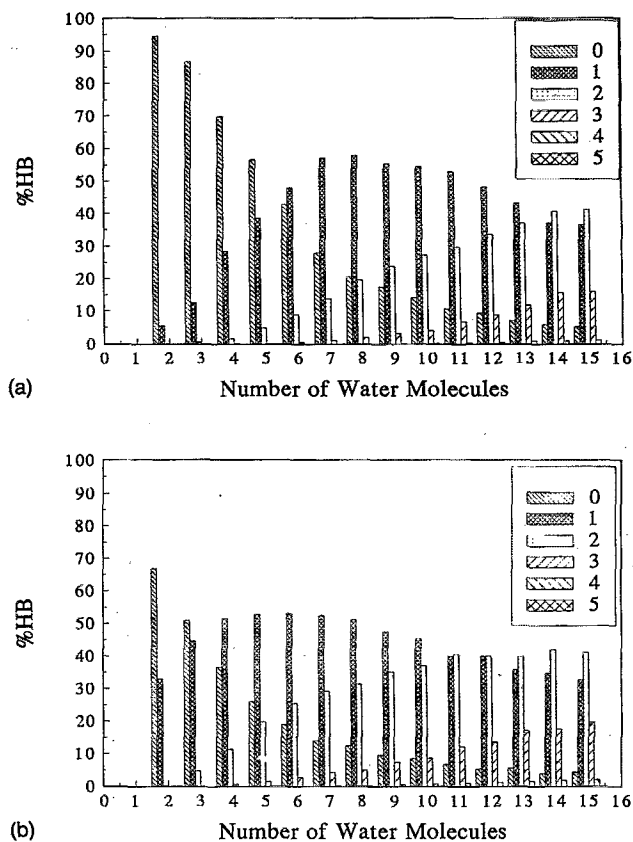
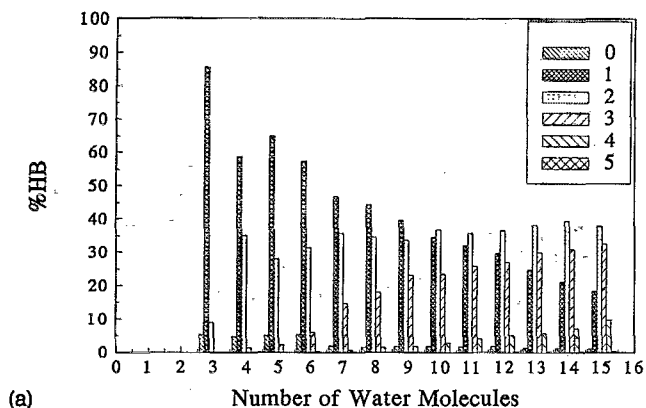


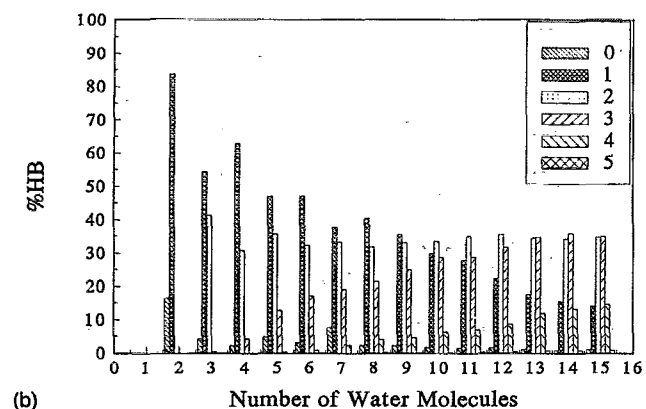
FIG. 7. (a) The percentage of 0, 1, 2, 3, 4, 5 hydrogen bonded water molecules in $\text{F}^-(\text{H}_2\text{O})_n$ clusters. The water molecules belong to the first hydration shell around the ion. We used the geometric criteria (see Ref. 38) to determine the presence of the hydrogen bonding. (b) The same as (a), only for $\text{Cl}^-(\text{H}_2\text{O})_n$ clusters.

shells when $n=10, 11, 12$; for clusters with $n=13, 14,$ and 15, the amount of water molecules with two hydrogen bonds per water is the same as with three hydrogen bonds. This again confirms that the hydrogen bonding network in water is stronger in clusters with Cl^- compared to the clusters where the F^- ion is solvated.

As we have mentioned in the introduction, the electrostatic stabilization energies obtained from the photodetachment spectra of $\text{Br}^-(\text{H}_2\text{O})_n$ and $\text{I}^-(\text{H}_2\text{O})_n$ ($n=1,2,\dots,15$) clusters can be scaled so that the data fall on a common curve. That means that Br^- and I^- ions are in similar environments in clusters with the same number of water molecules. From our previous discussions on Cl^- and F^- we have to conclude that since the F^- ion is solvated in water clusters and the Cl^- ion is not, the stabilization energies of these two ions in water clusters cannot be brought to the same curve by a simple scaling. Indeed, this is confirmed in Fig. 9, where we display the calculated values of the electrostatic stabilization energies. The detailed description of how such calculations are done is given in our previous paper.²⁷ Let us note here that the values of E_{stab} are experimentally measured for $\text{Cl}^-(\text{H}_2\text{O})_n$ ($n=1,2,\dots,7$) clusters (our calculations are in good agreement with these measurements), while no data are available for the clusters with the F^- ion. Therefore only future



(a)



(b)

FIG. 8. (a) The percentage of 0, 1, 2, 3, 4, 5 hydrogen bonded water molecules in $\text{F}^-(\text{H}_2\text{O})_n$ clusters. The water molecules belong to the second and third hydration shells around the ion. (b) The same as (a), only for $\text{Cl}^-(\text{H}_2\text{O})_n$ clusters.

experimental work on the photodetachment spectra for larger sized clusters with the Cl^- ion and on clusters with the F^- ions in water will show how accurate our calculations are.

Very often the cluster structures are discussed in terms of minimum energy structures and transitions between these minimum energy structures. For small atomic clus-

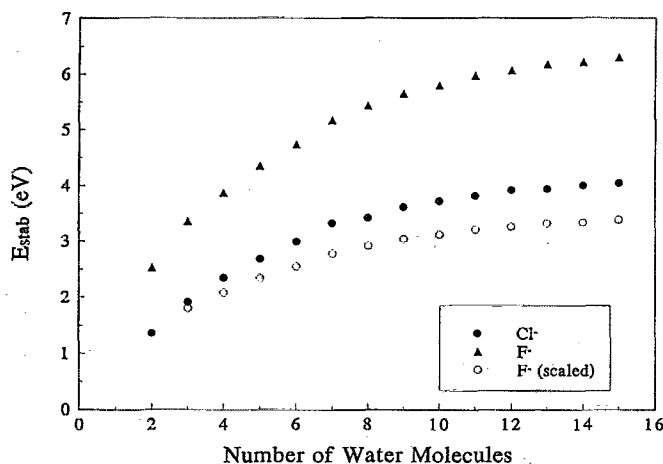


FIG. 9. Electrostatic stabilization energies for the $\text{Cl}^-(\text{H}_2\text{O})_n$ and $\text{F}^-(\text{H}_2\text{O})_n$ ($n=2,3,\dots,15$) clusters.

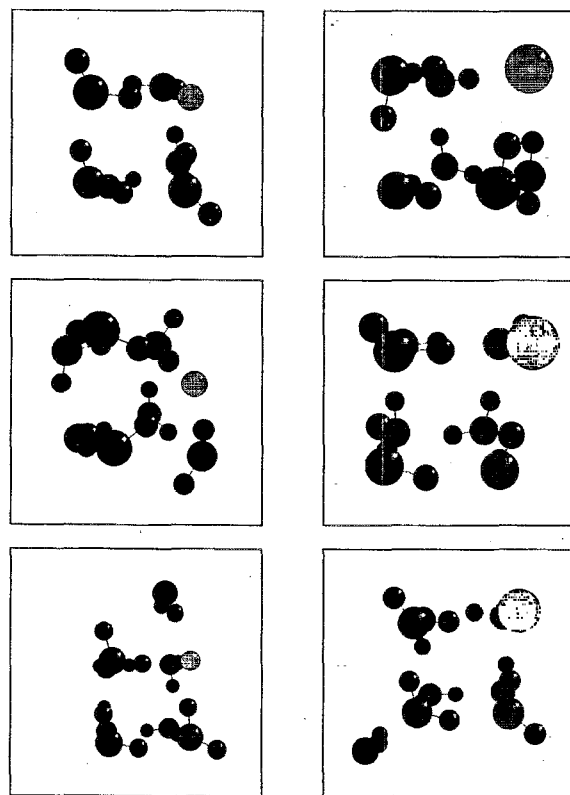


FIG. 10. $\text{F}^-(\text{H}_2\text{O})_n$ and $\text{Cl}^-(\text{H}_2\text{O})_n$ ($n=6,7,8$) clusters in their minimum energy configurations. On the left are the clusters with the F^- ion and on the right are clusters with the Cl^- ion. The upper row depicts clusters with $n=6$, the middle row $n=7$, the lower row $n=8$.

ters this method can give a complete picture of the structure and dynamics in clusters, since one can find all local minima of the clusters.³⁴ For molecular clusters a comprehensive search for all local minima are quite impossible. Nevertheless it is very interesting to know how the structure of the cluster in its global energy minimum looks like, since this is the structure the cluster would have at $T=0$ K. Comparison of this structure with the structures at $T\sim 250$ K can give us an idea how important the energy and the entropy components of the free energy are in determining the cluster structures at $T\sim 250$ K. To find the local energy minima for some of our clusters we quenched 500 structures from molecular dynamics trajectories of the clusters $\text{Cl}^-(\text{H}_2\text{O})_n$ and $\text{F}^-(\text{H}_2\text{O})_n$ ($n=6,7,8$). The starting points for quenching were separated by 2 ps. The quenching was performed using the conjugated gradient method. In Fig. 10 we represent the lowest energy structures that we obtained from our quenching procedures. To understand the geometry of these clusters, we have to remember that the minimum energy structure of a cluster with eight water molecules is a cube.³⁵ As we can see from Fig. 10, the structure of a cluster $\text{Cl}^-(\text{H}_2\text{O})_7$ is also a cube, where Cl^- substituted one of the water molecules at the vertex of the cube. We can see also that the structure of other clusters can be also understood as being derivatives of the basic cubic structure. As always, it is hard to know if our structures represent the global minima, but the sim-

ilarity of the structures to the cubic structure of the established global minimum indicate that our structures are close to the global minimum structures. Figure 10 also shows that both F^- and Cl^- ions prefer to be on the surface of the minimum energy clusters with 6, 7, and 8 waters. But as our molecular dynamics simulations show, at $T \sim 250$ K the F^- ion is found inside the clusters, while Cl^- still remains on the surface [see Figs. 5(a) and 5(b)]. That means that at least in clusters with 6, 7, and 8 waters the solvation of the F^- ion is due to the entropy effect. A more detailed study of minimum energy structures of water clusters with anions is now underway.

IV. CONCLUSIONS

We have performed molecular dynamics calculations on $\text{Cl}^-(\text{H}_2\text{O})_n$ and $\text{F}^-(\text{H}_2\text{O})_n$ ($n=2,3,\dots,15$) clusters. These calculations show that the F^- ion is solvated in the clusters with $n>4$, while Cl^- remains attached to the water in the clusters. In our previous work we used the argument of similarity to show that the I^- and Br^- ions are also attached to the water in the clusters. Very recently a direct molecular dynamics calculation of I^- in water clusters showed that the I^- ion is on the surface of the cluster.³⁶ Our calculations of the clusters with the Br^- ion also show that the ion is on the surface of the cluster.³⁷

Based on our calculations presented above and on our previous calculations we conclude that the F^- ion is solvated in clusters with $4 < n < 15$ water molecules, while larger size halide anions are not solvated in this size clusters. Why then is F^- solvated in water clusters while larger size halide anions are just attached? To answer this question let us assume that the water molecules in the cluster do not want to disrupt their hydrogen bonded network. One needs a rather strong perturbation to do this. Such perturbation may be produced by the F^- ion, because it is smaller in size than the other halogen ions and therefore the electric field around it has a larger value. But even then the perturbation may not be strong enough [as we saw from minimum energy structures for $\text{F}^-(\text{H}_2\text{O})_n$ ($n=6,7,8$)] and therefore the solvation of the ion is due to the entropy effect.

One can ask a question related to the reliability of our potential functions used in the simulations. As we have demonstrated above the calculations with these functions reproduce rather well enthalpies of formation of small $\text{F}^-(\text{H}_2\text{O})_n$ and $\text{Cl}^-(\text{H}_2\text{O})_n$ clusters. Moreover the electrostatic stabilization energies in small $\text{Cl}^-(\text{H}_2\text{O})_n$ ($n=1,2,\dots,7$) clusters are also reproduced. The electrostatic stabilization energies of Br^- and I^- ions that we can calculate from the molecular dynamics simulations can be compared with the experiment for clusters with up to 15 water molecules. Unfortunately this is not the case for the clusters with Cl^- and F^- ions. Therefore, more experimental data are needed to confirm our conclusions about the behavior of Cl^- and F^- ions in water clusters.

Note added in proof: We have recently learned that *ab initio* calculations performed on $\text{F}^-(\text{H}_2\text{O})_n$ ($n=1,\dots,6$) clusters³⁹ are in agreement with our conclusion that the

distribution of surface and interior states are temperature dependent.

ACKNOWLEDGMENTS

This work was supported by a grant from the Office of Naval Research. We are grateful to Professor O. Chesnovsky for providing us with the data on Cl^- and Br^- ions prior to their publication. The critical reading of the manuscript by L. S. Sremaniak and by the anonymous referee is acknowledged.

- ¹I. Dzidic and P. Kebarle, *J. Phys. Chem.* **74**, 1466 (1970).
- ²M. Arshadi, R. Yamdagni, and P. Kebarle, *J. Phys. Chem.* **74**, 1475 (1970).
- ³U. Nagashima, H. Shinohara, N. Nishi, and H. Tanaka, *J. Chem. Phys.* **84**, 209 (1986).
- ⁴K. Hiraoka and S. Mizuse, *Chem. Phys.* **118**, 457 (1987); K. Hiraoka, S. Mizuse, and S. Yamabe, *J. Phys. Chem.* **92**, 3943 (1988).
- ⁵X. Yang and A. W. Castleman, Jr., *J. Am. Chem. Soc.* **111**, 6845 (1989).
- ⁶X. Yang and A. W. Castleman, Jr., *J. Phys. Chem.* **94**, 8500 (1990).
- ⁷S. Wei, Z. Shi, and A. W. Castleman, Jr., *J. Chem. Phys.* **94**, 3268 (1991).
- ⁸A. Selinger and A. W. Castleman, Jr., *J. Phys. Chem.* **95**, 8442 (1991).
- ⁹D. R. Zook and E. P. Grimsrud, *Int. J. Mass Spectrom. Ion Processes* **107**, 293 (1991).
- ¹⁰G. Markovich, R. Giniger, M. Levin, and O. Chesnovsky, *J. Chem. Phys.* **95**, 9416 (1991).
- ¹¹F. Misaizu, T. Kondow, and K. Kuchitsu, *Chem. Phys. Lett.* **178**, 369 (1991).
- ¹²F. Misaizu, K. Tsukamoto, M. Sanekata, and K. Fuke, *Chem. Phys. Lett.* **188**, 241 (1992).
- ¹³T. P. Lybrand and P. A. Kollman, *J. Chem. Phys.* **83**, 2923 (1985).
- ¹⁴S. Lin and P. C. Jordan, *J. Chem. Phys.* **89**, 7492 (1988).
- ¹⁵L. A. Curtiss and R. Jurgens, *J. Phys. Chem.* **94**, 5509 (1990).
- ¹⁶E. N. Brodskaya and A. I. Rusanov, *Mol. Phys.* **71**, 567 (1990).
- ¹⁷I. Rips and J. Jortner, *J. Chem. Phys.* **97**, 536 (1992).
- ¹⁸J. E. Combariza, N. Kestner, and J. Jortner, *Chem. Phys. Lett.* **203**, 423 (1993).
- ¹⁹S. S. Xantheas and T. H. Dunning, Jr., *J. Phys. Chem.* **96**, 7505 (1992).
- ²⁰T. Asada, K. Nishimoto, and K. Kitaura, *J. Phys. Chem.* **97**, 7724 (1993).
- ²¹L. X. Dang, J. E. Rice, J. W. Caldwell, and P. A. Kollman, *J. Am. Chem. Soc.* **113**, 2481 (1991).
- ²²J. W. Caldwell, L. X. Dang, and P. A. Kollman, *J. Am. Chem. Soc.* **112**, 9145 (1990).
- ²³L. X. Dang, *J. Chem. Phys.* **96**, 6970 (1992).
- ²⁴J. V. Coe, G. H. Lee, J. G. Eaton, S. T. Arnold, H. W. Sarkas, K. H. Bowen, C. Ludewigt, H. Haberland, and D. R. Worsnop, *J. Chem. Phys.* **92**, 3980 (1990).
- ²⁵R. N. Barnett, U. Landman, and A. Nitzan, *J. Chem. Phys.* **89**, 2242 (1988).
- ²⁶The photodetachment spectra on I^- in water clusters with up to 15 water molecules were published in Ref. 10. Photodetachment spectra of Br^- in water clusters with up to 15 waters and of Cl^- with up to 7 waters were provided to us by Professor O. Chesnovsky. We extracted from these spectra the values for the electrostatic stabilization energies which were presented in Ref. 27.
- ²⁷L. Perera and M. L. Berkowitz, *J. Chem. Phys.* **99**, 4222 (1993).
- ²⁸In Ref. 27 and in the present paper we report the results of our calculations done on $\text{X}^-(\text{H}_2\text{O})_n$ clusters when the smallest number of water molecules in the cluster is $n=2$. We observed that the calculated photodetachment spectra for the ion and one water molecule displayed pronounced asymmetry, perhaps due to the ion and water locking into a long living complex. Therefore our results were dependent on the initial configurations when we studied the $\text{X}^-(\text{H}_2\text{O})$ complex.
- ²⁹J. W. Caldwell and P. A. Kollman, *J. Phys. Chem.* **96**, 8249 (1992).
- ³⁰L. Perera and M. L. Berkowitz, *J. Chem. Phys.* **95**, 1954 (1991). In part of the simulations, described in this paper we, by mistake, assigned an incorrect charge to the water hydrogen when we worked with the TIP4P potential. For a more detailed description of the changes in the

- calculations with the TIP4P potential see erratum [J. Chem. Phys. **99**, 4236(E) (1993)].
- ³¹L. Perera and M. L. Berkowitz, J. Chem. Phys. **96**, 8288 (1992).
- ³²L. Verlet, Phys. Rev. **98**, 159 (1967).
- ³³J. P. Ryckaert, G. Ciccotti, and H. J. C. Berendsen, J. Comput. Phys. **23**, 327 (1977).
- ³⁴F. G. Amar and R. S. Berry, J. Chem. Phys. **85**, 5943 (1986).
- ³⁵C. J. Tsai and K. D. Jordan, J. Chem. Phys. **95**, 3850 (1991).
- ³⁶L. X. Dang and B. C. Garrett, J. Chem. Phys. **99**, 2972 (1993).
- ³⁷L. S. Sremaniak, L. Perera, and M. L. Berkowitz, Chem. Phys. Lett. (in press).
- ³⁸M. Mezei and D. L. Beveridge, J. Chem. Phys. **74**, 622 (1981).
- ³⁹J. E. Combariza and N. R. Kestner, J. Phys. Chem. (in press).